NASA TECHNICAL MEMORANDUM

NASA TM X-73588

NASA TM X-73588

FLAP NOISE AND AERODYNAMIC RESULTS FOR MODEL QCSEE OVER-THE-WING CONFIGURATIONS

by W. Olsen, R. Burns, and D. Groesbeck
Lewis Research Center
Cleveland, Ohio 44135

TECHNICAL PAPER to be presented at the
Fifteenth Aerospace Sciences Meeting sponsored by the
American Institute of Aeronautics and Astronautics
Los Angeles, California, January 24-26, 1977

FLAP NOISE AND AERODYNAMIC RESULTS FOR MODEL QCSEE OVER-THE-WING CONFIGURATIONS

by W. Olsen, R. Burns, and D. Groesbeck

National Aeronautics and Space Administration
Lewis Research Center
Cleveland, Ohio 44135

E-9051

ABSTRACT

Noise spectra in three dimensions and aerodynamic data were measured for a model of the NASA QCSEE (Quiet Clean Short-Haul Experimental Engine) over-the-wing configuration. The effects of flap length, nozzle exhaust velocity, and nozzle geometry were determined using a single nozzle and wing-flap segment.

Related tests indicated that the scaled-up model data would be representative of full scale flap noise with the QCSEE engine. The scaled-up QCSEE model data imply that the noise goal will be very nearly attained.

INTRODUCTION

The primary objective of the Quiet Clean Short-Haul Experimental Engine (QCSEE) program is the development of technology for two types of STOL aircraft engines. These engines would be used to augment lift; one is mounted under-the-wing (UTW) and the other over-the-wing (OTW). The noise associated with the lift augmentation is one of the dominant noise sources for the QCSEE powered aircraft (ref. 1).

As part of the research effort for QCSEE program at the Lewis Research Center, aerodynamic and noise measurements were taken for a model of the nominal OTW QCSEE configuration. The first objective was to determine if the aircraft powered by QCSEE engines would meet the 95 EPNdB noise goal (ref. 1). The second objective was to determine the effect of nozzle configuration, jet velocity, and flap length on the flow and noise. The noise data were also compared with the predictions of a current flap noise prediction model; a similar comparison was made in reference 2 for a UTW configuration.

Free field noise spectra in three dimensions were measured for 1/28 and 1/11.5 scale models of the nominal OTW configuration and variations of that configuration. Related tests were also performed to insure that the scaled up model data would be representative of the full scale flap noise with the QCSEE OTW engine. Static aerodynamic measurements, such as velocity profiles, lift, and thrust, were also obtained.

STAR category 07
AIAA Paper No. 77-23

Aerodynamic Data

Static lift and thrust measurements were taken on the aerodynamic facility described in reference 5. Velocity profiles were obtained on this facility at the nozzle exit plane and also at the trailing edge of the wing-flap test model. These measurements were made with a traversing pitot-static tube aligned with the flow, and were automatically plotted on graph paper.

Description of the QCSEE Configurations Tested

A scale drawing of the QCSEE nominal configuration is given in figure 2(a). The nozzle and wing-flap design was based on "state of the art" information. The nozzle is essentially a "D" shaped nozzle with side doors. The side doors are opened during takeoff and approach for better flow attachment on the wind-flap surface, and also to match engine cycle area requirements. The nominal flap configuration used for approach is shown by D, and A shows the nominal flap position and length for takeoff. The takeoff flap angle, ψ , is 30°, and 75° is used for approach.

A 1/11.5 scale model of this nominal nozzle geometry (designated herein as N1) was built by the Langley Research Center for aerodynamic tests in a wind tunnel (ref. 6). Acoustic tests were conducted with this model at an outdoor acoustic rig at the Lewis Research Center. The engine core (see fig. 2(a)) was not simulated (i.e., not included) for either of these test series. The height, h, of the nozzle was 8 cm and the wing-flap span was about 11 nozzle heights wide. The roof internal angle, β, was 23 1/2°, and the side door angle was 25°. Additional flap lengths were also tested as shown in Table 1.

A 1/28 scale model was also built for additional acoustic (anechoic chamber) and aerodynamic static tests (site of ref. 5) at Lewis. This small model (5.2 cm equivalent diameter) is shown on figure 2(b). Several wing-flap lengths and nozzle geometries were tested with this model, as shown on figure 2(b) and Table 1. The wing-flaps were very nearly geometrically similar to the nominal configuration shown on figure 2(a). These tests used the N2 and N3 nozzles, which had different roof angles, β, of 23 1/2 and 28°, respectively. The height, h, of the N2 nozzle was 3.3 cm, and 3 cm was the height of the N3 nozzle. The N2 nozzle geometry was very close to that of the N1 nozzle geometry, except for the floor of the nozzle. The bottom of the 1/28 scale model nozzles (N2 and N3) was the wing surface. Therefore, unlike the N1 nozzle (nominal configuration), the small spanwise flow through the side doors encountered no step The nozzle was centered on the wing flap which was about 9.2 nozzle widths wide.

Additional OTW Configurations

Additional model aerodynamic and acoustic tests were performed to insure that the data from the small model tests was representative of

full scale engine data. These tests involved a scaling law test and a high velocity core simulation test.

In the scaling law test acoustic and aerodynamic data were obtained for a geometrically similar 1/18.5 scale model of the full scale OTW configuration (using a TF-34 engine, ref. 7). The configuration is shown on figure 3; it involved a canted slot nozzle (4:1 aspect ratio) over a wing with a short flap. The exhaust from the nozzle was uniform. The model tests duplicated the nozzle exhaust velocities and microphone angles of the engine tests; and both sets of data were free field and lossless.

The core of the QCSEE OTW engine (see fig. 2(a)) has no forced mixer. Therefore, the high velocity core jet exhausts from the engine exit nozzle unmixed. The QCSEE model tests had a uniform exhaust velocity. A test was performed to determine if a high velocity core jet would modify the results from the model tests that had a uniform exhaust velocity. The high velocity core jet was simulated by the following. A fine screen, (with a 1.8 cm dia hole in it) was placed inside of the 1/28 scale model nozzle. The core/fan velocity ratio and the relative core area of the engine were matched in this simulation. Velocity profiles, mass flow, lift, and noise spectra were measured.

Test Procedure

Far field acoustic data and aerodynamic data were taken separately on the facilities described above at a number of ideal nozzle exhaust velocities, V_n, ranging from about 150 to 275 m/sec. The nozzle and flap configurations tested are shown in figure 2 and table 1. The aerodynamic data were taken with the 1/28 scale model configurations, and the acoustic data were taken using both the 1/28 and 1/11.5 scale model configurations.

RESULTS AND DISCUSSION

The results are discussed in three major sections. The first section deals with the aerodynamic and acoustic results for the model scale QCSEE configurations. The second section involves aerodynamic and acoustic tests designed to determine whether the model data are representative of full scale engine data. In the third section, the perceived noise level is computed from the model scale data and compared with the QCSEE flap noise goal.

QCSEE Configurations

Aerodynamic results. - Velocity profiles and lift and thrust measurements, taken with the 1/28 scale model configurations shown on figure 2(b) and table 1, are discussed in this section.

Velocity measurements. - Constant velocity contours were obtained in the spanwise plane passing through the trailing edge of the flap and normal to the flap surface there. These contours are shown on figure 4(a) for the nominal length takeoff flap (A) at a nozzle velocity, V_n, of 720 ft/sec. The contours show that the flow is well attached to the flap. Compared with an OTW configuration using a circular nozzle with deflector (ref. 8), the QCSEE nozzle shows very little spanwise or axial decay of the velocity.

The peak velocity occurs at the center of the span ($z = 0$). The velocity profile at the center of the span was obtained from these contour data and is plotted on figure 4(b). Profiles are also shown for other takeoff flap lengths. These results indicate that the peak trailing edge velocity is about 99 percent of the nozzle velocity for the short flap, 95 percent for the nominal length and 89 percent for the long flap. These profiles also indicate that attachment was good for all takeoff flaps but not for the approach flap. The results on figure 4 are for the N2 nozzle; essentially the same results were obtained with the N3 nozzle with its steeper roof angle.

Velocity profiles were also obtained at the model nozzle exit plane. These profiles were uniform and in agreement with the ideal velocity, V_n, calculated from the nozzle pressure ratio and temperature.

Lift-thrust measurements. - A polar plot of the static lift and thrust results for a number of nozzle and flap configurations is shown on figure 5. The takeoff flap (30° flap angle) data are clustered near a turning angle of 30° for several flap lengths, nozzle shapes, and velocities. This indicates close flow attachment. The short flap turned the flow somewhat less than the long and nominal flaps.

The approach flap (75° flap angle) had bad flow attachment, it turned the flow only 55°. Comparable results were obtained in Langley experiments (ref. 9) with the 1/11.5 scale model (fig. 2(a)).

The turning efficiency for all flaps increased as the velocity was increased. This is not shown on figure 5; but, as benchmark, the nominal velocity data are indicated by solid symbols. The static turning efficiency at the nominal velocities was about 0.83 for the takeoff flaps and 0.77 for the approach flap. The lift and thrust were normalized to an ideal thrust ($\rho V_n^2 A_n$), where ρ and V_n were calculated from the pressure ratio and temperature. The area of the nozzle, A_n, is the open area of the nozzle with the doors open, except that the area of the side door openings is excluded (see fig. 2). This exclusion is reasonable because only about 5 percent of the flow passes through the side openings, which account for about 20 percent of the total nozzle area. If the ideal thrust was based on the measured flow and ideal velocity, the efficiencies for the takeoff and approach flaps would have been 0.9 and 0.81, respectively. Similar static tests were performed at Langley with the

1/11.5 scale model and the approach flap (ref. 9). Nearly the same turning efficiency was noted when the results were compared on the same ideal thrust basis.

Acoustic Results

The noise data presented in this section are summarized in figures 6 to 11. For those requiring more detail, complete tables of the three dimensional spectral sound emission are available on request.

Method of data presentation. - For convenience, the three dimensional spectral sound emission from the QCSEE OTW configuration is presented as follows. The data are separated into two quantities

$$\Delta SPL = SPL - OASPL_{\theta_i, \varphi} \tag{1}$$

$$OASPL_{\theta_i,\varphi} = OASPL_{\theta_i,\varphi=0} + \Delta\varphi \tag{2}$$

The first quantity, ΔSPL, describes the shape of the spectra, which tends to be a function of only the configuration, azimuth angle φ and the Strouhal number, S

$$S = fd_e/V_n \tag{3}$$

The second quantity (eq. (2)) describes the OASPL radiation patterns in the θ_i and φ coordinate directions (see fig. 1). The radiation pattern in the $\varphi = 0^\circ$ plane is described by $OASPL_{\theta_i,\varphi=0}$ while $\Delta\varphi$ describes the azimuthal change from the $\varphi = 0^\circ$ pattern as φ is increased.

It is convenient to break up $OASPL_{\theta_i,\varphi=0}$ into three terms.

$$OASPL_{\theta_i,\varphi=0} = \underbrace{10 \log_{10} \left(\frac{A_n}{R^2} \frac{V_n^n}{T_o^3} \right)}_{\text{Scaling}} + \underbrace{K}_{\substack{\text{Configu-} \\ \text{ration} \\ \text{constant}}} + \underbrace{\Delta_{\theta_i}}_{\substack{\text{Shape of} \\ \text{radiation} \\ \text{pattern}}} \tag{4}$$

The first term accounts for the model size (i. e., the nozzle area, A_n), microphone distance (R), environmental temperature (T_o), and the nozzle exit flow velocity (V_n). This term is used to scale up the SPL level of model data to full size. The second term, K, is a configuration constant. The third term is the shape of the radiation pattern in the $\varphi = 0^\circ$ plane at some V_n. For many configurations, the shape of the radiation pattern does not change with velocity (e. g., the exponent, n = 6.7 for multi-flap UTW config-

urations at all θ_i).

OASPL level and radiation patterns. - The OASPL radiation patterns in the $\varphi = 0^o$ plane are plotted on figure 6 for the 1/11.5 scale model with the N1 nozzle. The measured patterns for the takeoff and approach flaps are plotted as data points on figures 6(a) and (b), respectively. Examination of these results indicates that the level and shape of the OASPL pattern are essentially the same for the takeoff and approach flaps, wherever $\theta_i < 100^o$.

Additional nozzles and flap lengths were also tested. It was observed that the shape of the radiation pattern was not significantly affected by changes in the flap length or nozzle configuration. However, the level was affected. For example, the OASPL at $\theta_i = 90^o$ varied with L/h according to $-27 \log_{10} L/h$ for the N1 and N2 nozzles. The N2 and N3 nozzles were 4 dB quieter than the N1 nozzle for all flap lengths.

The data shown on figure 6 were compared[1] with the results (shown as the smooth curves) from the UTRC flap noise prediction model (ref. 10). This model is a noise component method where a number of sources and effects are accounted for semi-empirically. The agreement between the data and model results is excellent over most of the polar arc. The poor agreement for those θ_i above the flap exhaust is not a major flaw in practice. Furthermore, the data near the flap exhaust were occasionally affected by flow impingement on those microphones; those data are, therefore, not reliable.

The azimuthal variation of the OASPL for the takeoff flap and velocity is shown in figure 7 at three polar angles. The quantity $\Delta\varphi$ is the difference between the OASPL measured at φ and the OASPL measured at $\varphi = 0^o$, which is shown on figure 6. The data at $\theta_i = 90^o$ for the takeoff flap show that the OASPL at $\varphi = 90^o$ is about 10 dB lower than the OASPL at $\varphi = 0^o$.

The data are compared with the UTRC prediction model[2] on figure 7. The data and the UTRC model agree for most of the polar arc.

---

[1]The calculations were performed by M. Fink, as part of NASA Contract NAS3-17863, without reference to the data in this paper.

[2]A trigonometric error was discovered in the UTRC model (ref. 10) by its author, it was corrected for this comparison. This error caused a poor agreement at $\theta_i < 60^o$ in a similar comparison (ref. 2) for an UTW configuration. After correcting the error, the agreement was improved.

Multi-flap UTW flap noise data (ref. 11) produced noise radiation patterns whose shape was unaffected by the velocity; the velocity exponent, n, in equation (4) was constant (n = angles θ_i and φ. The shape of the OASPL patterns shown on figure 6 changes with velocity. This implies that n is not independent of θ_i for the QCSEE OTW configuration. Figure 8 shows the variation of the velocity exponent, n, with θ_i for several flap lengths and azimuth angles, φ.

The data indicates that the exponent varies from n = 6., at small θ_i, to n = 8, at large θ_i. At $\theta_i = 90^\circ$, n = 7. There is no systematic variation of n with φ, nozzle shape, or flap length. The result from the UTRC model is close to the average of the data.

SPL spectra. - The SPL spectra at $\theta_i = 90^\circ$ for the nominal configuration are shown in figure 9 for several azimuth angles. Figure 9(a) is for the nominal takeoff flap at the takeoff velocity, while figure 9(b) is for the approach flap and velocity. The reduction in SPL with increasing φ is much larger at low frequency than at high frequency. The perceived noise level (PNL), calculated directly from these type of spectra, is given in the last section of this paper.

These free field spectra are not smooth at low frequency. This lack of smoothness has also been noted in free field data for a multi-flap UTW configuration (ref. 2), and also in reference 12.

Data for the spectral shape of the takeoff flap noise at $\varphi = 0$ and $\varphi = 85^\circ$ are plotted on figures 10(a) and (b). In making these figures the SPL are normalized by the OASPL and plotted as a function of Strouhal number. The data shown are for several polar angles and velocities, and for various nozzle shapes and sizes. The data scatter ±2 dB about the average smooth curves drawn through the data (solid curve).

The spectral shapes for the approach flap at $\varphi = 0^\circ$ and 85° are shown on figures 11(a) and (b), respectively. These data also collapsed well about the smooth (solid) curves through the data. These curves are the same as used on figure 10, however the curve for $\varphi = 0^\circ$ had to be shifted to lower frequency by 1/3 octave.

For comparison, the spectral shapes from the UTRC prediction are also drawn on figures 10 and 11. The prediction agreed with the averaged smooth curves thru the data, except for figure 10(a) and at low frequency. The spectral shapes from the UTRC model are an average of the spectra predicted for the range of polar angles and velocities of the data. The variation of the spectra given by the UTRC prediction was small, which is consistent with the data.

Engine and Scaling Effects

The exhaust flow from the previously discussed model-scale

nozzles was uniform and at ambient temperature; and the initial turbulence was very low. In contrast, the exhaust flow from the QCSEE engine is expected to be highly turbulent with a prominent high velocity peak due to the unmixed hot core jet. This section describes the results from two experiments that were designed to show the effect of the above differences, and the accuracy of scaling. The first experiment determines the accuracy of scaling data from a geometrically similar 1/18.5 scale model of a TF-34 engine experiment that used a canted slot nozzle OTW configuration (ref. 7). The engine exhaust stream was turbulent; the model was not. Both the engine and model nozzle exhaust velocity profiles were uniform. The second experiment was performed to determine if the non-uniform exhaust (i.e., the high velocity core) of the QCSEE OTW engine would alter the aerodynamic and acoustic results obtained with a uniform velocity profile.

Accuracy of OTW model data scaling. - A full scale OTW configuration, using a TF-34 engine, canted slot nozzle and a short flap, was tested previously (ref. 7). These full scale results were about 6 dB higher than the scaled up OTW model data. This discrepancy could be due to the fact that the model data used was obtained with a configuration that was not geometrically similar to the full-scale configuration.

Acoustic and aerodynamic data were, therefore, obtained for a geometrically similar 1/18.5 scale model of the short flap, canted nozzle configuration used in that TF-34 engine test (see fig. 4). The model tests duplicated the engine velocities and microphone angles; and both sets of data were free field and lossless. The principal differences were related to scaling effects (e.g., the size and microphone distance) and the turbulence level at the nozzle exit plane of the engine (e.g., more than 10 percent for the engine compared to less than 1 percent for the model). Another difference, believed to be minor, was the exhaust temperature (180°C for the engine compared to 10° C for the model).

Velocity contours similar to those shown on figure 4(a) were measured for both the engine and model. Both sets of data were in excellent agreement.

The full scale spectra measured at $\theta_i = 90^\circ$ with the TF-34 engine (ref. 7) are plotted in figure 12 as solid symbols for two velocities. The scaled up spectra for the geometrically similar 1/18.5 scale model of the full scale configuration are plotted on figure 12 as open symbols. The agreement is excellent. The agreement at other polar angles (not shown) was equally good. Excellent agreement has also been shown previously in those few comparisons where geometrical similarity was carefully maintained (e.g., 3 flap UTW in ref. 2, and 2 flap UTW in ref. 13).

These results imply that data from small geometrically similar models will scale up to full scale to an accuracy approaching the accuracy of the data (±1 dB).

The span of the wing-flap segment for the TF-34 engine was 2.75 nozzle widths. The width was sufficient to insure there was no flow off the sides of the wing. Model experiments with flap spans of 2.75 and 6.7 nozzle widths showed that there was no span effect on the acoustic results in the $\varphi = 0^{o}$ azimuth plane. The flap span/nozzle width ratio of the model QCSEE experiments was 9.2 for the 1/28 scale models and 5.7 for the 1/11.5 scale models. Measurements were not taken at other azimuth angles.

Effect of high velocity core. - The predicted flow from the QCSEE engine has a prominent unmixed hot high velocity core jet. The QCSEE model and TF-34 scaling tests used nozzles which had a uniform nozzle exhaust velocity. The high velocity core of the QCSEE nozzle could possibly affect the accuracy of scaling up the model QCSEE acoustic and aerodynamic data to the full scale engine test. The experiments described in this section are "worst case" experiments to determine if the high velocity core could have an appreciable effect.

An analysis was performed (ref. 14) which indicated that the high velocity core engine jet (fig. 2(a)) would not noticeably mix by the time it reached the nozzle exit plane, regardless of whether the core jet was hot or cold. The lower density of hot core jet would of course result in faster mixing than a cold core jet as the flow passes over the flap. In order to determine if the high velocity core would affect the accuracy of scaling, a "worst case" experiment using a cold core flow was employed. A fine screen, with a hole in it, was placed inside of the 1/28" scale model nozzle to simulate the high velocity core jet of the engine core nozzle (see sketch in fig. 13 and fig. 2(a)). The hole was equivalent to the core nozzle area. Measurements downstream of the screen indicated that the largest (worst case) core to fan velocity ratio for the engine (1.6) was closely simulated.

Velocity contours were measured at the nozzle exit and at the trailing edge. A prominent sharp peak in the velocity contours, which is associated with the high velocity core, was observed at the nozzle exit plane. Although somewhat less prominent, it was also evident in the velocity contours measured at the trailing edge for the approach and takeoff flaps. Although this peak might affect the flow attachment, the trailing edge contours indicated flow attachment was unaffected. Lift and thrust measurements also indicated that the turning angle of the flow for the takeoff and approach flaps was the same as those observed with a uniform nozzle exhaust flow (see fig. 5). The static lift was compared at the same flow weighted velocity for the uniform and high velocity core cases. The static lift was very nearly the same.

The effect of a high velocity core on the noise produced is shown on figure 13. The "worst case" high velocity core case is compared with the uniform flow case at the same flow weighted velocity. In this case, this comparison is equivalent to a comparison made at the same static lift. According to reference 15, a comparison at the same static lift is a reasonable approximate way to make an acoustic comparison at the same performance level. The spectra are the same at the two values of static lift (or flow weighted velocity) where the comparisons were made.

Apparently the prominent peak in the trailing edge velocity contours is of insufficient size to noticeably affect the acoustic or aerodynamic results. In any future comparisons between the model data reported here and full scale results using the QCSEE engine, it is suggested that the comparison be made at the same flow weighted velocities. The model must also be geometrically similar to the full scale configuration.

PNL Results

The small model acoustic data reported in the first section were scaled up to describe the noise for a full scale QCSEE configuration with a single engine. The results are presented in this section. The perceived noise level, PNL, is computed and compared with the flap noise goal.

The noise goal (ref. 1) for the QCSEE aircraft is 95 EPNdB along a 150 m sideline. According to reference 1, the maximum EPNdB will occur when the aircraft is at an altitude of about 60 m ($\varphi = 67^{o}$) during takeoff or approach. The 95 EPNdB noise goal for the aircraft in flight is equivalent to a flap noise PNL requirement of 91.5 PNdB for free field data measured along a 150 m sideline distance in a full scale static experiment using a single QCSEE engine. The adjustment from the 95 EPNdB goal to the 91.5 PNdB flap noise requirement involves several contractually specified corrections. These corrections involve: other noise sources, four engines, engine thrust, fuselage shielding, flight effects, extra ground attenuation, ground reflection of the flight test site.

The model SPL spectra, measured in the $\varphi = 63^{o}$ azimuth plane, were scaled up according to equations (3) and (4). The SPL level of the model spectra were decreased 6 1/2 dB to account for the differences noted in table 2 (i.e., size, distance, and small differences in: φ, velocity and ambient temperature). The effect of high velocity core of the engine was accounted for by using a mass averaged velocity. The frequency of the model data was multiplied by the scale factor to obtain the full scale frequency. The 1/11.5 scale model data at 20 KHz is equivalent to a full scale frequency of only 1.6 KHz. A PNL calculation requires a spectrum up

to 10 kHz; an extrapolation of the model spectra is, therefore, required. A straight line extrapolation was used because it describes the high frequency model and full scale data (e. g., see figs. 9 and 12). The spectrum was then corrected for atmospheric attenuation and the PNL was calculated. It turns out that atmospheric attenuation at the high frequencies is so large that any inaccuracy in the extrapolation does not noticeably affect the value of PNL obtained.

The peak PNL along a 150 m sideline distance in the $\varphi = 63^{o}$ plane occurred at $\theta_i = 90^{o}$, as shown in figure 14 for the nominal takeoff conditions. The peak PNL occurred at $\theta_i = 90^{o}$ for all azimuth angles, velocities, and configurations tested. As a consequence, all subsequent PNL comparisons will be made at $\theta_i = 90^{o}$.

Effect of nozzle configuration. - The peak PNL ($\theta_i = 90^{o}$) was calcualted for several full scale QCSEE nozzle configurations (see table 1 and fig. 2) at the nominal velocities and flap lengths. Table 3 lists these results. The PNL values for the N2 and N3 nozzles, which differ slightly in the roof angle, were about the same, just below the 91.5 PNdB flap noise requirement at takeoff. The nominal configuration using the N1 nozzle was about 4 PNdB noisier than the requirement. The N1 and N2 nozzle geometries are similar except that the N1 nozzle has a step at the side door openings (compare figs. 2(a) and (b)). The N2 geometry was also tested with thick side doors (not shown); this was also about 4 PNdB noisier than the requirement. These results imply that the acoustic results are sensitive to the geometry of the nozzle. The flap noise at approach conditions was about 88 PNdB.

Effect of velocity and flap length. - The peak PNL was calculated at four velocities for several full scale nozzle and flap configurations. These results are plotted on figure 15 for the N1 and N2 nozzles with the nominal takeoff flap. The peak PNL follows a V_j^9 power law at $\varphi = 63^{o}$ and also at other azimuth angles. Therefore, a small reduction in the engine exhaust velocity will have a large effect on the perceived noise.

The effect on flap length on the PNL for the takeoff flap is shown in figure 16. The PNL would be reduced 1 PNdB for an 8 percent increase in the flap length from the nominal length. This result is substantially independent of the azimuth angle, velocity or nozzle configuration.

CONCLUDING REMARKS

The PNL of a full scale configuration using an engine can be predicted from scaled up small scale model data, or from analytical predictions. The accuracy of these methods is discussed here to

illustrate a few points.

It was previously demonstrated that scaled up data from a small geometrically similar model accurately reproduced full scale OTW results taken with the TF-34 engine to within 1 PNdB, which is approximately equal to the scatter of the data.

The PNL for the full scale QCSEE configuration can also be determined from the smooth averaged curves drawn through the mass of data on figures 6, 7, and 10. The PNL for takeoff was 93.7 PNdB with the N1 nozzle. This is 1.3 PNdB below the 95 PNdB value shown on table 3 for the N1 nozzle. The values in table 3 were calculated directly from the single spectra (measured at the desired conditions) with no averaging or smoothing. This difference gives another indication of the effect of data scatter and the non-smoothness of the spectrum.

The prediction from the UTRC model resulted in 92 PNdB. According to table 3 in the PNL for the N1 nozzle was 95 PNdB while N2 and N3 nozzles resulted in 90.5 and 91 PNdB. The predicted PNL results lie between the PNL bounds measured for the various nozzles. The UTRC prediction model could not predict such a large sensitivity to nozzle shape. Because of this configuration sensitivity, any future evaluation of analytical flap noise prediction models should be done with data from several significantly different flap configurations.

CONCLUSIONS

The following conclusions are based on the previous results.

1. Scaling and high velocity core tests indicated that scaled up model data would be representative of the full scale flap noise with the QCSEE engine. However, the model must be geometrically similar to the engine nozzle, and the high velocity core of the engine must be accounted for by using a flow weighted velocity.

2. The scaled up model flap noise data imply that the nominal QCSEE OTW configuration will very nearly meet the noise goal.

3. The flap noise level is sensitive to the geometry of the nozzle.

SYMBOLS

A_n	open area of nozzle excluding the side door opening, m^2
d_e	equivalent diameter of nozzle, m^2
f	frequency or center frequency of third octave band, Hz
h	nozzle height, m
K	configuration constant, dB
n	velocity exponent
R	microphone radius, m
S	Strouhal number, fd_e/V_n
SPL	sound pressure level, dB
T_o	environment temperature, ^oC
V	local velocity, m/sec
V_n	nozzle velocity, m/sec
y	perpendicular distance above trailing edge, m
z	spanwise distance from center of span, m
β	roof angle from nozzle centerline, deg
Δ_{θ_i}	$OASPL_{\theta_i} - OASPL_{\theta_i=90^o}$, dB
Δ_{φ}	$OASPL_{\theta_i,\varphi} - OASPL_{\theta_i,\varphi=0^o}$, dB
ΔSPL	SPL - OASPL, dB
θ_i	polar angle, measured from nozzle centerline at inlet, deg
ρ	density, kg/m^3
φ	azimuth angle of microphone plane from plane through centerline and perpendicular to wing surface, deg
ψ	flap angle from centerline, deg

REFERENCES

1. Loeffler, I. and Smith, E., "Acoustic Design of the QCSEE Propulsion Systems," Powered-Lift Aerodynamics and Acoustics (Proj. FEDD.). NASA SP-406, 1976, pp. 335-356. (Available from NASA Regional Dissimination Centers only to U.S. Requestors)

2. Fink, M. R. and Olsen, W. A., "Comparison of Predictions and Under-the-Wing EBF Noise Data," AIAA Paper 76-501, Palo Alto, Calif., 1976.

3. Olsen, W., "Noise Generated by Impingement of a Turbulent Jet on Isolated Airfoils of Varied Chord, Cylinders, and Other Flow Obstructions," AIAA Paper 76-504, Palo Alto, Calif., 1976.

4. Bass, H. and Shields, F., "Atmospheric Absorption of High Frequency Noise and Application to Fractional-Octave Bands," NASA CR-2760, 1976.

5. von Glahn, U. and Groesbeck, D., "Effect of External Jet-Flow Deflector Geometry on OTW Aero-Acoustic Characteristics," AIAA Paper 76-499, Palo Alto, Calif., 1976.

6. Quiet Clean Short-Haul Experimental Engine (QCSEE), Over-the-Wing (OTW), Final Design Report. Proposed NASA Contractor Report.

7. Heidelberg, L. G., Homyak, L., and Jones, W. L., "Full-Scale Upper Surface-Blown Flap Noise," SAE Paper 750609, Hartford, Conn., 1975.

8. Dorsch, R., Reshotko, M., and Olsen, W., "Flap Noise Measurements for STOL Configurations Using External Upper Surface Blowing," AIAA Paper 72-1203, New Orleans, La., 1972.

9. Phelps, A., "Static and Wind-On Tests of an Exhaust Nozzle for the QCSEE USB Engine," Proposed NASA Technical Memorandum.

10. Fink, M. R., "Prediction of Externally Blown Flap Noise and Turbomachinery Strut Noise," NASA CR-134883, 1975.

11. Olsen, W., Dorsch, R., and Miles, J., "Noise Produced by a Small-Scale Externally Blown Flap," NASA TN D-6636, 1972.

12. von Glahn, U. and Groesbeck, D., "OTW Noise Correlations for Variations in Nozzle/Wing Geometry with 5:1 Slot Nozzles," NASA TM X-73425, 1976.

13. Dorsch, R. G., Goodykoontz, J. H., and Sargent, N. B., "Effect of Configuration Variation on Externally Blown Flap Noise," AIAA Paper 74-190, Washington, D.C., 1974.

14. Povenelli, L., Personal Communication, NASA-Lewis, Cleveland, Ohio.

15. Kadman, Y. and Hayden, R., "Exploratory Study of EBF Noise Reduction Through Nozzle/Flap Positioning," BBN-2894, Bolt Geranek & Newman, Inc., Cambridge, Mass., 1976.

TABLE 1

OTW CONFIGURATIONS TESTED

Nozzle description	Scale	Roof angle, θ, deg	Flap angle, ψ, deg	Flap length, L/h	Comments
1. QCSEE tests (nominal config.)					
N1	1/11.5	23.5	30 (T.O.) 30 (T.O.) 30 (T.O.) 75 (App.) 75 (App.)	Nom. (A) 6.2 Long (B) 8.6 Short (C) 5.3 Nom. (D) 6.8 Langley 6.8	
N2	1/28	23.5	30 (T.O.) 30 (T.O.) 30 (T.O.) 75 (App.)	Nom. (A) 6.4 Long (B) 8.8 Short (C) 5.2 Nom. (D) 6.8	Also thick door test.
N3	1/28	28	30 (T.O.) 75 (App.)	Nom. (A) 7 Nom. (D) 7.5	Also high velocity core simulation tests.
2. Scaling test Canted 4:1 slot	1/18.5	----	40 (T.O.)	Short 6.9	Model of TF-34 configuration (ref. 7). Also short span test.

TABLE 2

SCALING PARAMETERS USED IN EQUATION (4) AND STROUHAL NUMBER

	Full Scale	Model Scale
Configuration	Single QCSEE Engine (400 KN Thrust)	Geometrically Similar Nozzle and Wing
Size (Scale Factor)	1	1/28 1/11.5
Azimuth Angle, φ	67^{o}	63^{o}
Distance, R	165 M at $\varphi = 67^{o}$ (150 M Sideline Distance)	3M 6M
Acoustic Data	Free Field	Free Field
Nominal Velocity, V_N	225 M/Sec (T.O.) 195 M/Sec (app.)	Almost the Same
Environment Temperature, T_0 Humidity	25^{o}C, 70 Percent } Standard Day	Varied

TABLE 3

PEAK PNL FOR VARIOUS QCSEE NOZZLE CONFIGURATIONS

At Nominal Velocities and Wing-Flap Lengths,

Full Scale Single Engine at 150 M Sideline Distance ($\varphi = 63^{o}$),

Free Field and Standard Day (25^{o} C, 70 Percent RH)

Configuration	PNL, PNdB
A. QCSEE Takeoff (225 M/Sec, Wing A)	
N1 Nozzle	95
N2	90.5
N3	91
B. QCSEE Approach (195 M/Sec, Wing D)	
N1	88.5
N3	88

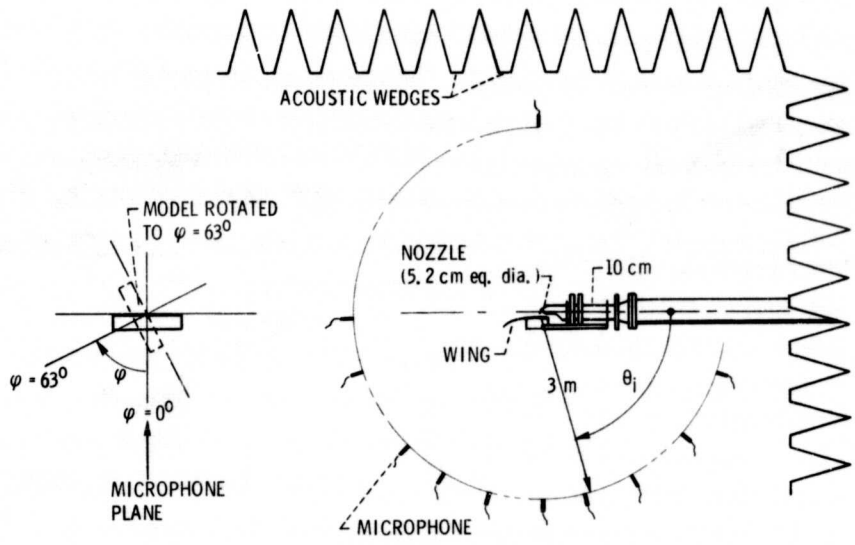

Figure 1. - Small test rig in Anechoic chamber.

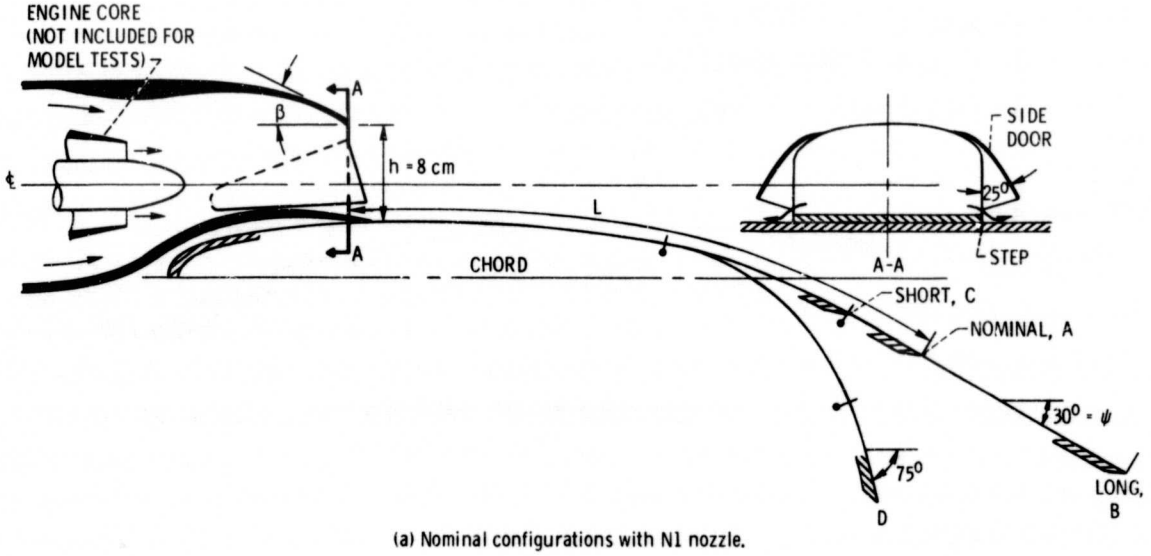

(a) Nominal configurations with N1 nozzle.

Figure 2. - QCSEE OTW Configurations.

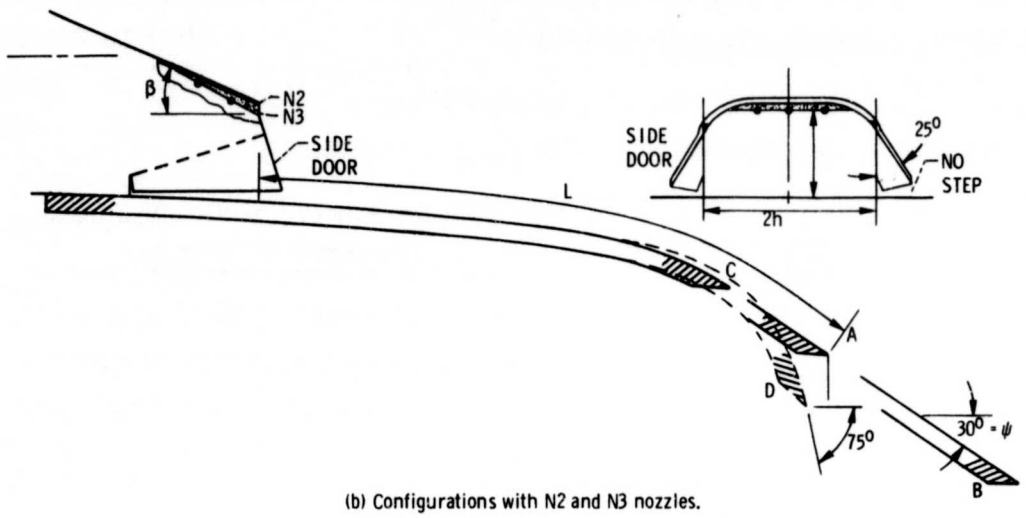

(b) Configurations with N2 and N3 nozzles.

Figure 2. - Concluded.

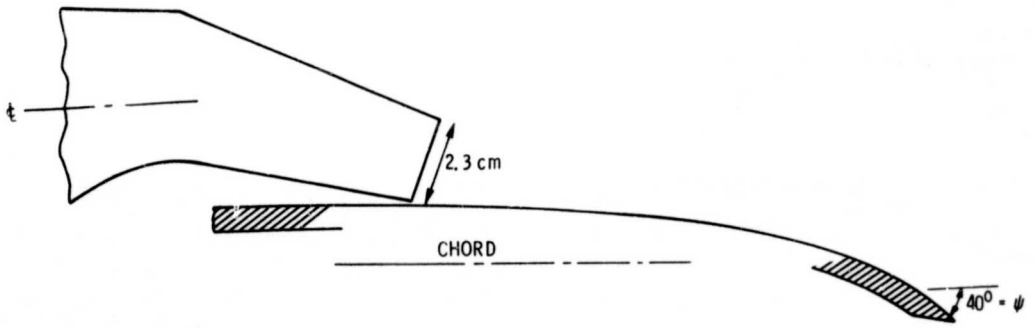

Figure 3. - Model of OTW configuration used in TF-34 engine test. Geometrically similar 1/18.5 scale model.

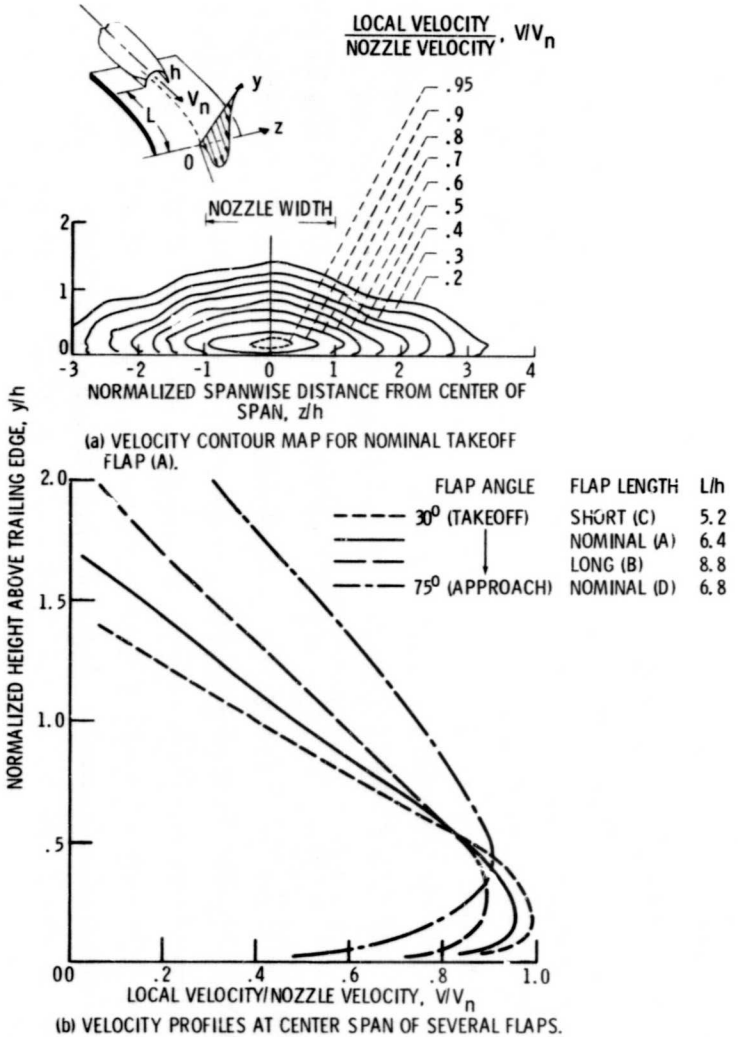

Figure 4. - Trailing edge velocity profiles. Nozzle velocity, V_n, 225 m/sec; 1/28th scale model with N2 nozzle; nozzle height, h, 3.3 cm.

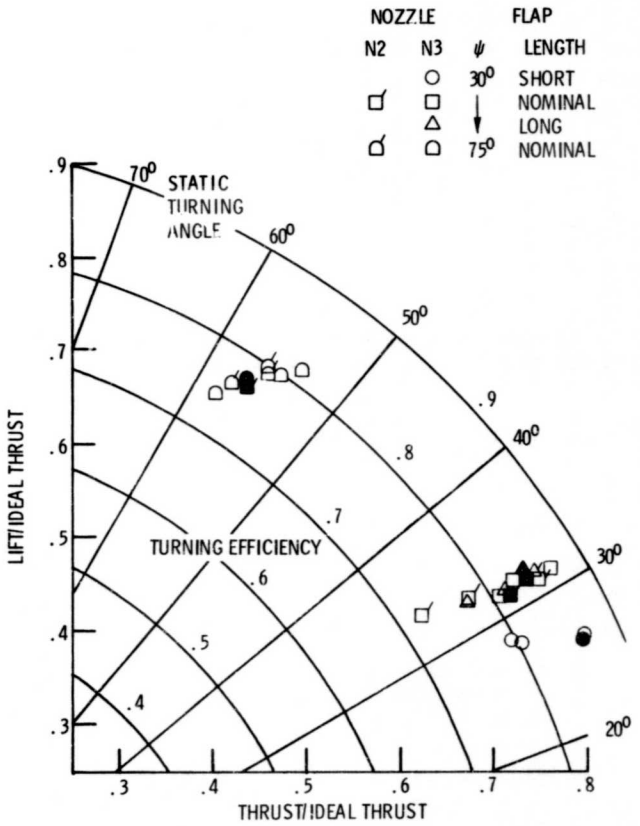

Figure 5. - Static turning effectiveness for several QCSEE configurations. Ideal thrust based on V_n and the nozzle open area without area of side openings, 1.9×10^{-3} m^2; 1/28th scale model with N2 nozzle, velocity range 150 to 275 m/sec.

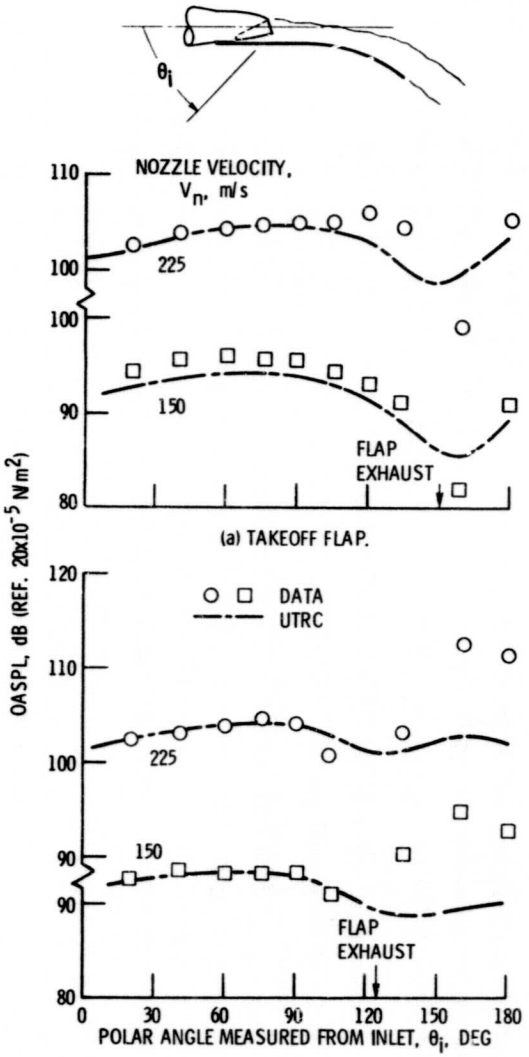

Figure 6. - OASPL radiation patterns. Azimuth angle, φ, 0^0; 1/11.5 scale model with N1 nozzle; microphone distance 6 m, environmental temperature, 25 C.

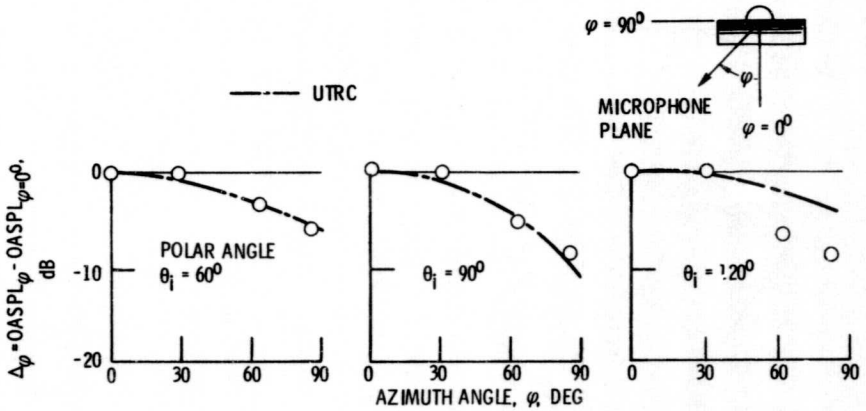

Figure 7. - Measured and calculated azimuthal variation in the OASPL takeoff condition: flap angle, ψ, 30^0 and nozzle velocity, V_n, 225 m/sec; 1/11.5 scale model with N1 nozzle.

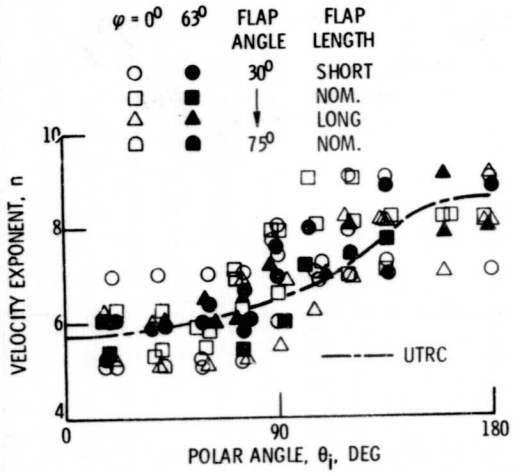

Figure 8. - Effect of polar angle, θ_i, on velocity exponent, n. Determined at constant θ_i from OASPL patterns measured over a velocity range of 140 to 275 m/sec. N1 nozzle.

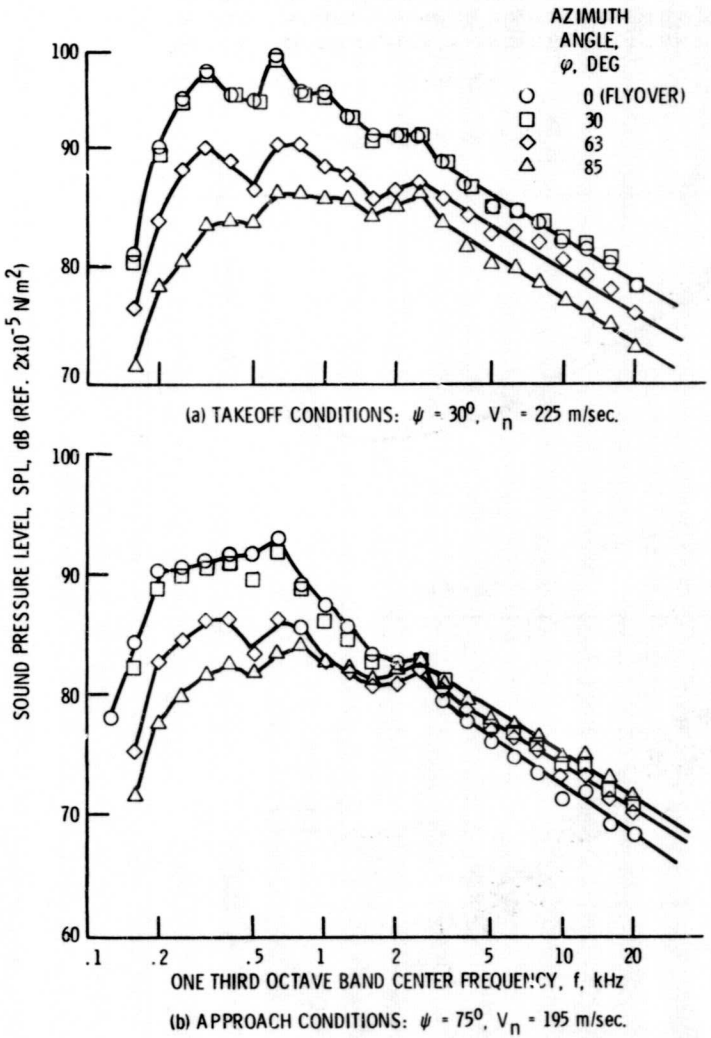

Figure 9. - Azimuthal variation of SPL spectra at $\theta_i = 90^0$. Nominal flap lengths; 1/11.5 scale model with N1 nozzle; free field lossless data taken at 6 m radius; environmental temperature, 25° C.

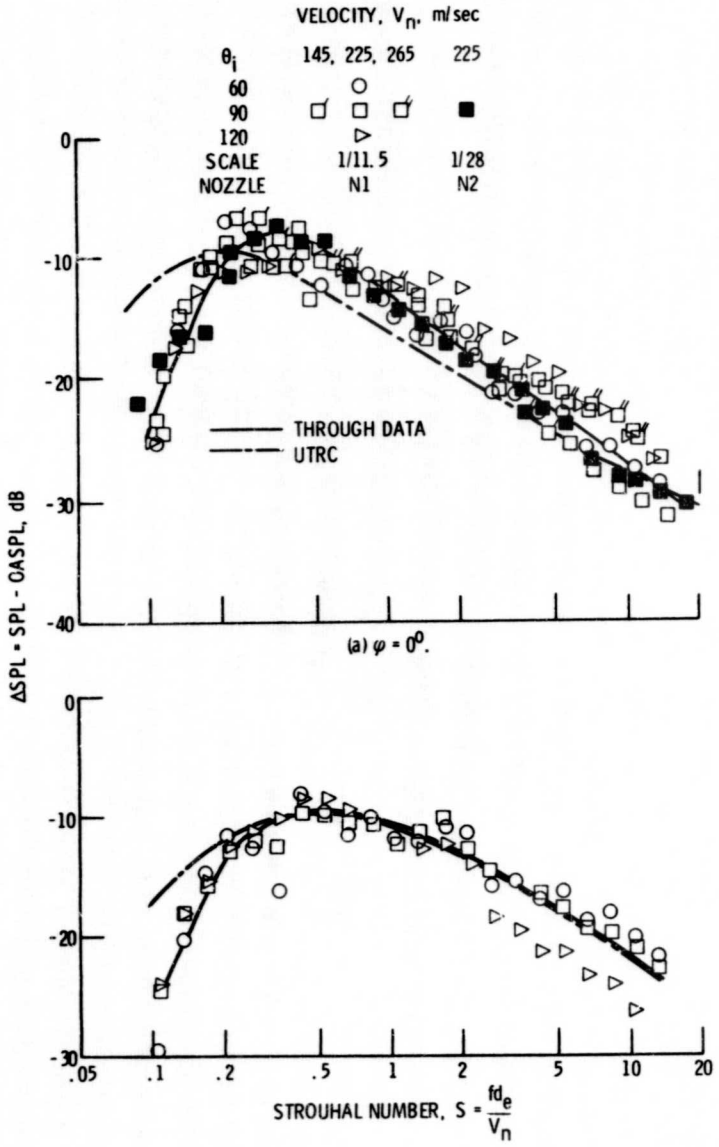

Figure 10. - Normalized spectra for takeoff flap over a range of polar angles and velocities. Nominal flap lengths; 1/11.5 and 1/28 scale models with N1 and N2 nozzle; free field lossless data.

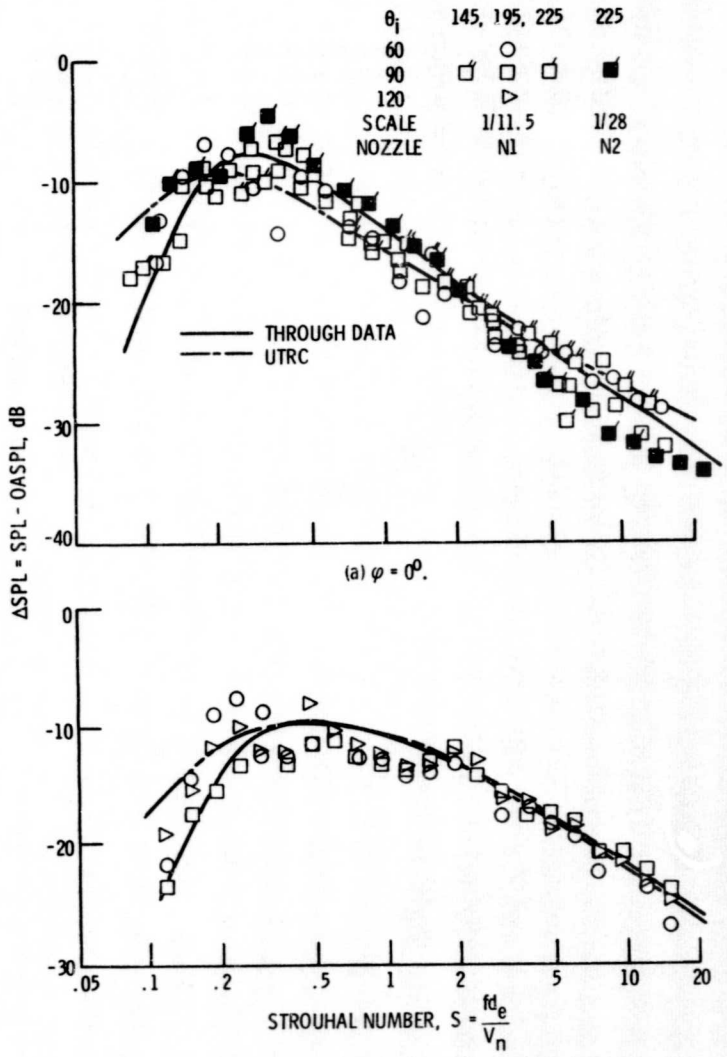

Figure 11. - Normalized spectra for approach flap over a range of polar angles and velocities. Nominal flap lengths; 1/11.5 and 1/28 scale models with N1 and N2 nozzles; free field lossless data.

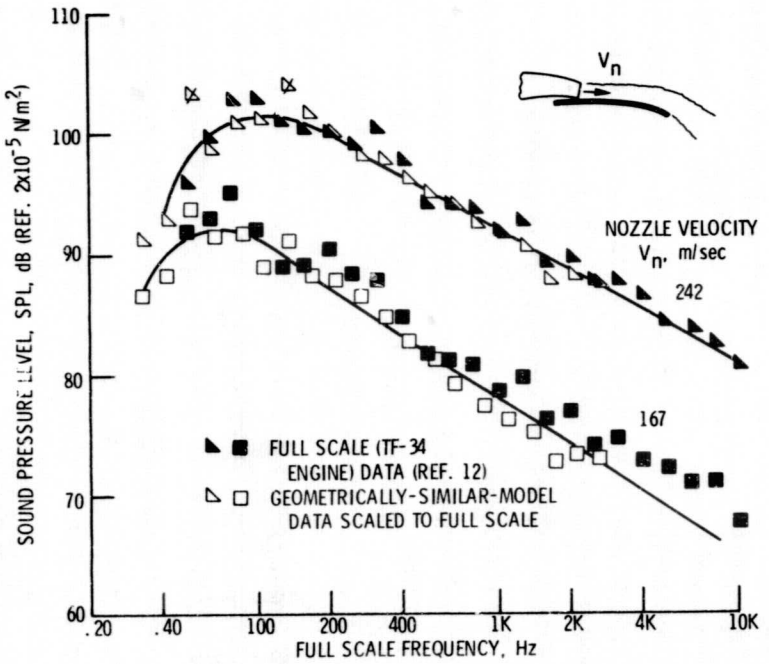

Figure 12. - Comparison of OTW model data to full size engine data. Polar angle, 90°; azimuth angle, 0°; distance, 100 ft; free field lossless data; environmental temperature, 25 C.

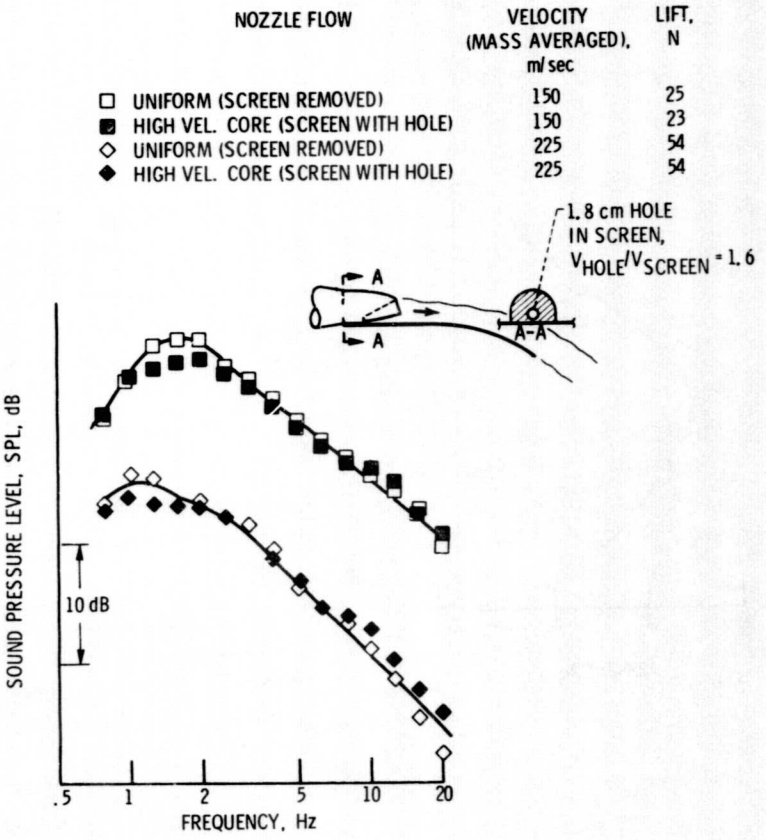

Figure 13. - Effect of high velocity core from QCSEE engine on noise. Engine velocity profile simulated by screen with core sized hole. Polar angle, 90°; azimuth angle, 0°, 1/28 scale model with N3 nozzle; nominal length takeoff flap.

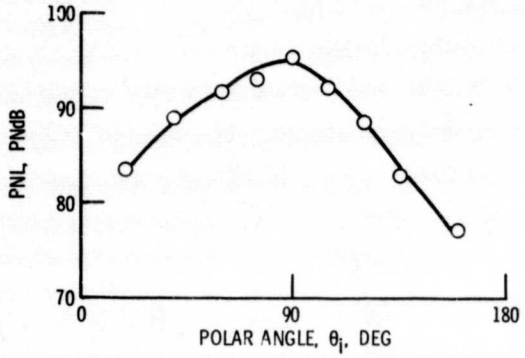

Figure 14. - Perceived flap noise level, PNL, along 150 m sideline for QCSEE OTW during takeoff. Azimuth angle, φ, 63°; nozzle velocity, 225 m/sec; nominal length takeoff flap; 1/11.5 scale model with N1 nozzle; standard day (25 C, 70% RH).

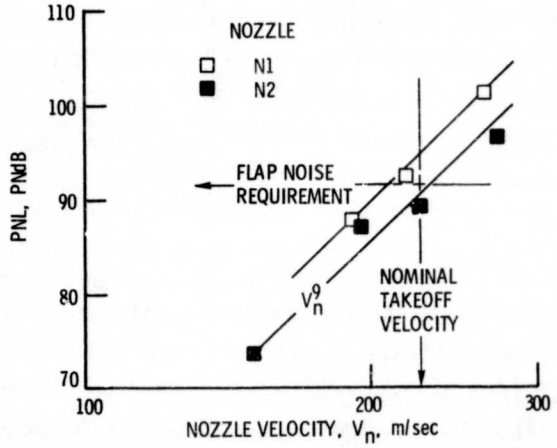

Figure 15. - Effect of velocity on peak PNL. Polar angle, θ_i, 90°; 150 m sideline at φ = 63°; nominal takeoff flap A; full scale single engine; standard day (25 C, 70% RH).

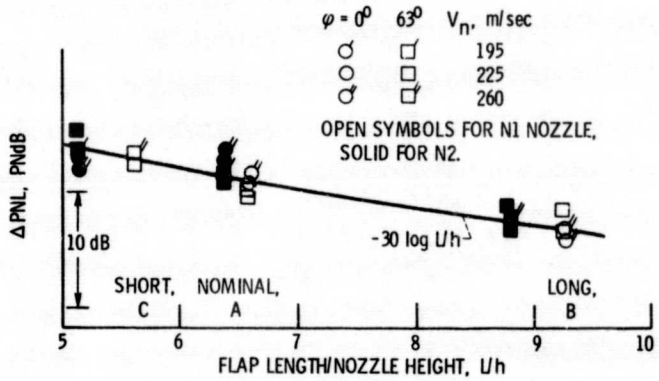

Figure 16. - Effect of flap length on PNL. Polar angle, θ_i, 90°; flap angle, ψ, 30°.

NASA-Lewis